2018

Bottom-quark fusion processes at the LHC for probing Z' models and B-meson decay anomalies

Mohammad Abdullah
Texas A&M University

Mykhailo Dalchenko
Texas A&M University

Bhaskar Dutta
Texas A&M University

Ricardo Eusebi
Texas A&M University

Peisi Huang
Texas A&M University, peisi.huang@unl.edu

See next page for additional authors

Authors
Mohammad Abdullah, Mykhailo Dalchenko, Bhaskar Dutta, Ricardo Eusebi, Peisi Huang, Teruki Kamon, Denis Rathjens, and Adrian Thompson

Bottom-quark fusion processes at the LHC for probing Z' models and B-meson decay anomalies

Mohammad Abdullah, Mykhailo Dalchenko, Bhaskar Dutta, Ricardo Eusebi, Peisi Huang, Teruki Kamon, Denis Rathjens, and Adrian Thompson

Mitchell Institute for Fundamental Physics and Astronomy, Department of Physics and Astronomy, Texas A&M University, College Station, Texas 77843, USA

(Received 3 August 2017; published 26 April 2018)

We investigate models of a heavy neutral gauge boson Z' coupling mostly to third generation quarks and second generation leptons. In this scenario, bottom quarks arising from gluon splitting can fuse into Z' allowing the LHC to probe it. In the generic framework presented, anomalies in B-meson decays reported by the LHCb experiment imply a flavor-violating bs coupling of the featured Z' constraining the lowest possible production cross section. A novel approach searching for a $Z'(\to \mu\mu)$ in association with at least one bottom-tagged jet can probe regions of model parameter space existing analyses are not sensitive to.

DOI: 10.1103/PhysRevD.97.075035

After the Higgs boson discovery [1,2], the major challenge for the LHC is to find new physics beyond the standard model (SM). Some intriguing excesses may hint at the presence of new physics. For instance, LHCb has reported an anomaly in the angular distribution of $B \to K^*\mu^+\mu^-$ [3,4] (A similar anomaly has also been reported by the Belle Collaboration [5]). These measurements have poorly understood hadronic factors [6] which, however, are less relevant for the LHCb measurements of R_K and R_{K^*}. Here R_{K^*} is defined as $\frac{\mathrm{BR}(B\to K^*\mu^+\mu^-)}{\mathrm{BR}(B\to K^*e^+e^-)}$ and R_K as $\frac{\mathrm{BR}(B^+\to K^+\mu^+\mu^-)}{\mathrm{BR}(B^+\to K^+e^+e^-)}$ and both show values lower than expected in the SM [7,8].

Combining R_K and R_{K^*}, the overall deviation from the SM expectation is at least at a level of 4σ [9,10]. A massive Z' with a flavor changing bs coupling, and a nonuniversal coupling to leptons could easily accommodate the R_K and R_{K^*} anomalies [11–38]. Such a new gauge boson is featured in many beyond the SM theories where an extra $U(1)$ group has been proposed [39–43]. Various models of Z' has been intensively searched for at the LHC, and the current limit is in the multi-TeV range [44–46]. While current Z' searches assume the Z' to couple to the first generation quarks and leptons, the current constraints on the Z' from LHC searches and B physics require the couplings to second and third generation fermions to be dominant.

We investigate a scenario that can satisfy the B-anomaly constraints in a dimuon final state. We will show that when the Z' boson couples to b quarks, it is possible to use the b's arising from gluon splitting with a final state consisting of at least one b-jet and two muons. As these diagrams are very similar to vector-boson fusion diagrams, we will name them bottom-fermion fusion (BFF) in the following. A generic framework of a minimal extension to the SM which explains the B anomalies is used to discuss the new search strategies in this BFF production process. This BFF production process allows us to interpret the inclusive dimuon searches in light of a Z' coupling to the third generation. We will show that the presence of additional b jets in the dimuon final state can be utilized to probe smaller Z' masses than the inclusive dimuon searches. This strategy can be utilized for any model where Z' couples to b quarks irrespective of solutions to B anomalies. We will show that the flavor violating bs coupling produces a lower bound on the Z' production cross section. We compare several signal hypotheses to the SM background showing the possibilities of probing the parameter space explaining the B anomalies at the present and future LHC runs.

The new physics contribution to rare B decays can be described by the following effective Lagrangian

$$\mathcal{L} \supset \frac{4G_F}{\sqrt{2}} V_{tb}V_{ts}^* \frac{e^2}{16\pi^2} C_9 O_9 + \mathrm{H.c.} \tag{1}$$

The effective operator O_9,

$$O_9 = (\bar{s}\gamma_\mu P_L b)(\bar{\mu}\gamma^\mu \mu), \tag{2}$$

describes a four-fermion interaction, with a left-handed $b - s$ current and a vector current for μ. To fit the current data [47], the new physics contribution to C_9 needs to be $-1.59^{+0.46}_{-0.56}$.

Here, we consider a toy model by extending the SM by adding an extra $U(1)$ gauge group, which introduces a new gauge boson Z'. With a flavor changing quark coupling and a nonuniversal lepton coupling, it can generate a contribution to the desired effective operator. The minimal phenomenological Lagrangian is

$$\mathcal{L} \supset Z'_\mu[g_\mu \bar{\mu}\gamma^\mu \mu + (g_b \delta_{bs} \bar{s}\gamma^\mu P_L b + \text{h.c.})] \tag{3}$$

The contribution to the effective O_9 operator is

$$\frac{e^2}{16\pi^2} V_{ts}^* V_{tb} C_9 = -\frac{v^2}{2m_{Z'}^2} g_b \delta_{bs} g_\mu. \tag{4}$$

which, using the central value of C_9, leads to the requirement

$$g_b \delta_{bs} g_\mu (100\ \text{GeV}/m_{Z'})^2 \simeq 1.3 \times 10^{-5} \tag{5}$$

To evade the current bounds from the LEP and the LHC, we consider a scenario where the $U(1)$ charges of the fermions are flavor dependent as done in many studies [16,18,22,48,49] to generate Eq. (3). The Z' to bs coupling may, for instance, be generated from the mixing of vector-like quarks and leptons with their SM counterparts. In the lepton sector, the Z' needs to couple only to the muons. In order to preserve $SU(2)$ invariance, the Z' also couples to tops and muon neutrinos. We can write the following dominant terms in the Lagrangian in a model which contains Eq. (1) and is allowed by all the existing constraints in order to address the anomalies:

$$\mathcal{L} \supset Z'^\mu \Big[g_\mu \bar{\mu}\gamma^\mu \mu + g_\mu \bar{\nu_\mu}\gamma^\mu P_L \nu_\mu + g_b \sum_{q=t,b} \bar{q}\,\gamma^\mu P_L q + (g_b \delta_{bs} \bar{s}\gamma^\mu P_L b + \text{h.c.}) \Big] \tag{6}$$

The Z' mass is constrained to be less than 5.5 (10) TeV in the 1 (2) sigma range to explain the B anomalies. It can be as light as 100 GeV while still satisfying B anomalies and other constraints [49]. As shown in Eq. (6), the Z' does not significantly couple to first or second generations quarks thus weakening current limits on Z' production at the LHC. However, the Z' can be produced through its couplings to b quarks originating either from sea quarks, or gluon splitting. Therefore, the Z' is associated either with two b-jets (both b quarks from gluon splitting), one b-jet (one b quark from each of gluon splitting and sea quarks), or no b-jet (both b quarks from sea quarks).

The Z' will decay into pairs of b quarks, muons, muon neutrinos, and, if kinematically allowed, top quarks. Therefore, the relevant final states at the LHC are dimuon or di-b resonances. The cross sections behave as follows:

$$\sigma(pp \to Z' \to \mu\mu) \propto 2g_b^2(1 + k\delta_{bs}^2) g_\mu{}^2 \tag{7}$$

$$\sigma(pp \to Z' \to b\bar{b}) \propto 3g_b^4(1 + k\delta_{bs}^2) \tag{8}$$

where k contains the s-quark PDF effect since the production of Z' may occur through bs fusion. When δ_{bs} goes to zero, the flavor conserving contribution dominates the production of Z'. When δ_{bs} is large but still satisfies the B anomalies (so smaller g_b) the flavor violating contribution dominates.

Since the Z' is produced primarily through b couplings and can decay into a pair of muons, bottom quarks, or tops, the searches for dimuon [44–46], dijet [50–52] or $t\bar{t}$ [53,54] resonances are relevant. The reliance on bottom quarks for production in our scenario weakens the impact of existing searches compared to scenarios utilizing production via first generation quarks. Dijet and $t\bar{t}$ constraints are inconsequential since the uncertainty in the $t\bar{t}$ cross section measurement is several pb and the current 8 TeV constraint on the resonance searches is $\mathcal{O}(\text{pb})$ while the dimuon resonance searches produce relevant constraints.

In addition to direct searches for a Z', its flavor changing coupling also generates a contribution to the $B_s - \bar{B}_s$ mixing, thereby changing the mass difference of B_s mesons. The current measurement of the deviation from the standard model is about $\Delta_{B_s} = 0.07 \pm 0.09$. [55]. For a Z' of $\mathcal{O}(100)$ GeV, the $B_s - \bar{B}_s$ mixing is the dominant constraint [49] while other flavor constraints, such as muon $g-2$ [56] and $\text{BR}(B \to K\bar{\nu}\nu)$ [57,58] are weak.

The measurement of neutrino trident production [59] places an upper bound on g_μ which, while too weak for our purpose, translates into a lower limit on the combination of $g_b\delta_{bs}$ that explains the B anomalies.

Since the measurements of R_K and R_{K^*} fix the combination $\frac{g_b \delta_{bs} g_\mu}{m_{Z'}^2}$, Z' production through BFF dominates for large g_b and, therefore, small δ_{bs} and g_μ. For each value of $m_{Z'}$ we will fix g_μ such that $g_b\delta_{bs}$ has the maximum value allowed by B_s mixing. When δ_{bs} becomes as large as about 0.6, diagrams including s-quarks start dominating the production of Z' and is not covered in this work.

Figure 1 shows the range of production cross-sections for dimuon $+\,b$ or 2 b final states for $m_{Z'} = 350$ GeV and $g_\mu = 0.13$ as a function of δ_{bs} with central (black line), 1 sigma (green shade region) and 2 sigma (yellow shaded region) fits of the B anomalies. The allowed cross-section band has a smaller slope for larger δ_{bs} due to the dominance of $g_b\delta_{bs}$ coupling initiated Z' production, whereas in the smaller δ_{bs} region, the Z' production is dominantly governed by the flavor conserving g_b term which decreases as δ_{bs} increases. For particular masses, the central fit (1σ range) minimum cross sections are 0.2(0.12) fb for

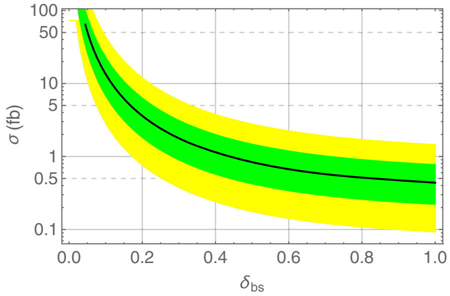

FIG. 1. Production cross section for a BFF dimuon resonance as a function of δ_{bs} for a 350 GeV Z' and $g_\mu = 0.13$ which satisfies the LHCb constraints. The central fit (black line) and the 1σ (green shaded region) and 2σ (yellow shaded region) contours of the B anomalies are shown.

$m_{Z'} = 500$ GeV, 0.6(0.2) fb for $m_{Z'} = 350$ GeV, and 1.2(0.8) fb for $m_{Z'} = 200$ GeV. Existing constraints are weak to constrain the parameters for $m_{Z'} \leq 350$ GeV due to the large SM background contributions in that region. The BFF production of the dimuon final state allows us to rule out a large region of parameter space. For this allowed parameter space, we introduce a simplified search strategy for various mass points searching for $Z' \to \mu\mu$ with at least $1b$ jet in this subsection.

For the following study of expected limits and selection requirements, we use MadGraph5 v.2.5.4 [60] to generate signal and background samples. We use a modified version of the FeynRules model file for the Hidden Abelian Higgs Model [61] as well as a model file of our own [62,63]. Pythia 8.2 [64] is used for parton showering and Delphes 3.4 [65] for the detector simulation with a default CMS card. We consider pileup effects to be mostly mitigated in a realistic experimental analysis, thus we did not include any. Electron and muon candidates are restricted to $|\eta| < 2.5$ and < 2.4, respectively. Jets are required to have $p_{\mathrm{T}} > 30$ GeV. The jet pair in our selection is always comprised of the leading b-tagged jet together with the next-to-leading jet that is b-tagged, if possible. Only if no second b-tagged jet with $p_T > 30$ GeV exists, the leading non-b-tagged jet in transverse momentum is chosen instead. A medium working point of the identification of b quark jets in the Delphes package is used, where the b-tagging efficiency is varying with p_{T} (65% at $p_{\mathrm{T}} > 30$ GeV) and the corresponding misidentification probability for gluon- and light-flavored quark jets is in the range of 1–2%.

For a normal search for a heavy resonance decaying to opposite sign (OS) dimuons, the main backgrounds are Drell-Yan and $t\bar{t}$ events. Requiring OS dimuons and at least two jets with $p_T > 30$ GeV, at least one of them passing a b-tag requirement, reduces Drell-Yan (+0,1,2 jets) process contributions to the search region by a factor of $\mathcal{O}(100)$. The remaining background in the mass range beyond the Z-boson peak is the di-leptonic $t\bar{t}$ process that we further suppress by a set of three selection requirements:

(1) Top mass bound $M_{\mu b}$: We examine the muon-jet invariant mass in both exclusive permutations out of the dimuons and the two jets (bb or bj). Of the two possible muon-jet parings, we choose the one with the smallest mass difference and require the heavier mass to be greater than 170 GeV.
(2) Leptonic versus hadronic activity: The scalar sum of transverse momenta of the leading OS muon pair (L_{T}) must be larger than the scalar sum of transverse momenta of the leading bottom-tagged pair or bottom and non-tagged jet pair (H_{T}).
(3) Normalized missing transverse energy ($E_{\mathrm{T}}^{\mathrm{miss}}$): The ratio of $E_{\mathrm{T}}^{\mathrm{miss}}$ to dimuon mass ($M(\mu^+\mu^-)$) is restricted to below 0.2 to reject events with real sources of $E_{\mathrm{T}}^{\mathrm{miss}}$.

While the top quark mass bound and the normalized $E_{\mathrm{T}}^{\mathrm{miss}}$ are expected to be useful for reducing di-leptonic $t\bar{t}$ contributions, the difference between L_{T} and H_{T} is specific to the BFF initial state. In contrast to forward-backward VBF production with its typical large invariant mass and rapidity gap selection on forward jets, BFF jets are usually centrally produced and, due to the gluon-splitting nature of their production, soft. This can be used to select BFF-produced heavy resonances in favor of many SM background scenarios that prefer more even distributions of transverse momenta without requiring the high momentum thresholds other initial states like boosted object searches necessitate. In addition, it is possible to use more stringent requirements on $H_{\mathrm{T}} - L_{\mathrm{T}}$ to generate even background-free selections for heavier resonance scenarios. The m_{T2} variable [66] has also been tested and found not to significantly improve on the other three selection requirements. As the best performance of inclusive dimuon resonance searches moves to higher masses as expected background contributions rise with increasing integrated luminosity, we expect more stringent selections like BFF to become competitive in terms of exclusion power for an increasing range of masses.

TABLE I. Efficiency of selection requirements for a simplified search for three different mass points assuming $\delta_{bs} = 0$ with a dimuon $t\bar{t}$ background. The requirements are applied successively from left to right. Each entry indicates the individual requirement's efficiency after applying all other selections in columns to its left. The total efficiency of a background is the multiplication of all entries in a given row.

	Preselection	$M_{\mu b}$	$H_{\mathrm{T}} - L_{\mathrm{T}}$	$E_{\mathrm{T}}^{\mathrm{miss}}/M(\mu^+\mu^-)$
$t\bar{t}$	8%	17%	26%	27%
SM Z	0.2%	41%	32%	54%
Z' 200	7%	60%	74%	89%
Z' 350	10%	82%	90%	97%
Z' 500	13%	90%	94%	98%

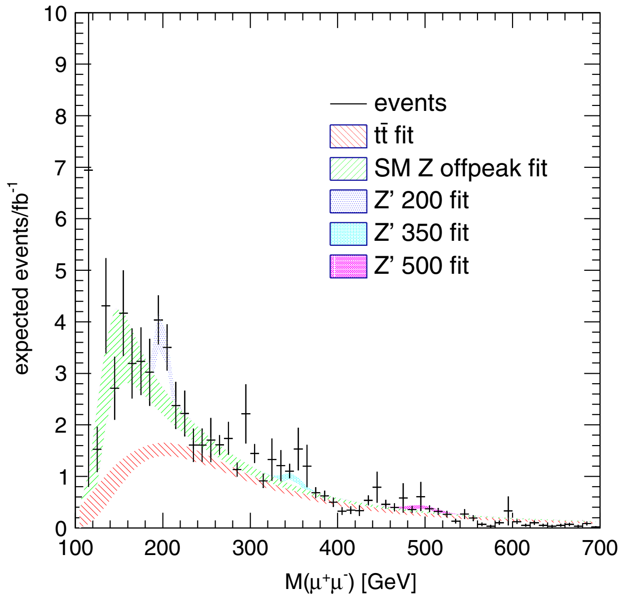

FIG. 2. Opposite sign dimuon invariant mass distribution for selected simulated events including the shape fits for background and signal contributions used to generate expected limits. Simulated data shows statistical uncertainties due to event weights only, uncertainty bands for the fits show the one sigma uncertainties of varying all fit parameters.

Table I contains the efficiencies of the aforementioned selection requirements on dileptonic $t\bar{t}$, SM Z and three different mass scenarios for the Z' model. The signal preselection is a function of δ_{bs} and Z' mass, as higher masses increase the hardness of associated jets and the centrality of events while higher values of δ_{bs} decrease the overall proportion of associated bottom jets compared to the total production cross section. We fit the dependence upon δ_{bs} with a linear fit for each mass point by generating several differently δ_{bs}-valued samples with constant g_b. Then, we fit the resulting absolute values of slopes and intercepts versus Z' mass with a logarithmic fit each to determine a function describing the signal acceptance A over the complete parameter space:

$$A(m_{Z'},\delta_{bs}) = (0.063 - 0.026\delta_{bs})\ln\left(\frac{m_{Z'}}{\mathrm{GeV}}\right) - 0.268 + 0.11\delta_{bs} \qquad (9)$$

Applying this selection yields Fig. 2. We use $g_\mu \sim 1$ to calculate the Z' decay width to make sure our bound is valid for such high values of couplings. The values dictated by the B anomalies are much smaller and would lead to a narrower width and hence a larger significance.

Utilizing this new search strategy, we show the LHC reach for 200, 350, and 500 GeV Z' masses in the $\delta_{bs} - g_b$ parameter space in Fig. 3 along with constraints from $B_s - \bar{B}_s$ mixing [49] and trident production [59]. The 1σ and 2σ contours of the best B anomalies fits are shown for the smallest g_μ values satisfying the mixing limits. The values of g_μ are 0.08, 0.14, and 0.20 for Z' masses of 200 GeV, 350 GeV, and 500 GeV respectively. The 95% exclusion limits for 30, 300 and 3000 fb^{-1} of LHC integrated luminosity using $2(1)b +$ dimuon final states are contrasted with the current and projected inclusive dimuon search limits [44,46]. Also shown are the regions excluded by neutrino trident production as explanations of B anomalies. Note that these latter limits are on g_μ which has no bearing $g_b\delta_{bs}$ if we do not require a fit to B anomalies.

For $m_{Z'} = 200$ GeV, a $2(1)b +$ dimuon search as proposed in this work is more efficient in mitigating the background than the inclusive dimuon analogue leading to

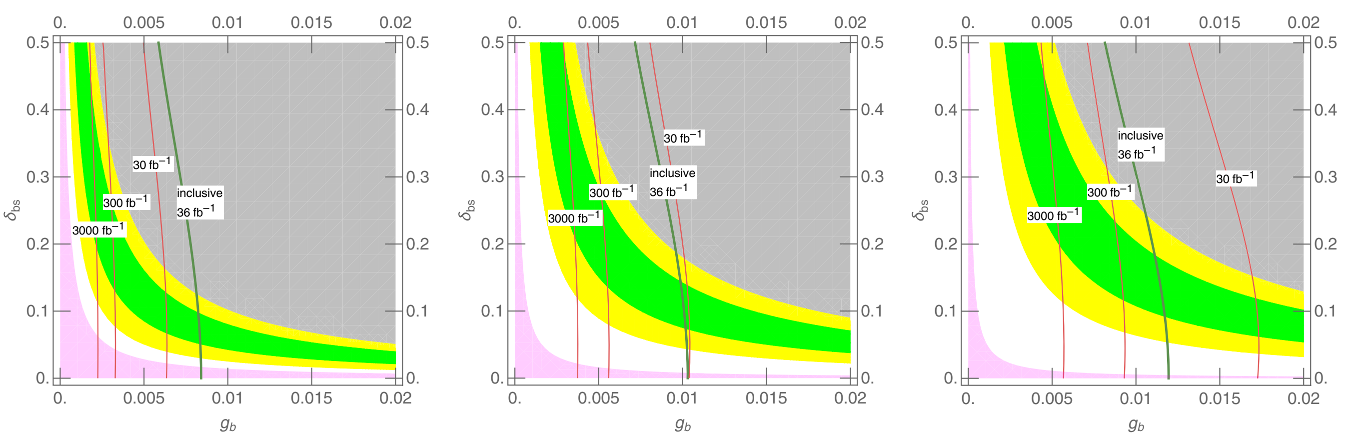

FIG. 3. The current and future expected LHC limits for various luminosities for three different Z' masses: 200, 350 and 500 GeV (left to right). Green lines refer to the current reach of an inclusive dimuon search while red lines show the expected power of a $2(1)b +$ dimuon search. The yellow and green shaded regions correspond to 2σ and 1σ bands of the best fit to the B anomalies for the chosen values of g_μ (0.08, 0.14 and 0.20 respectively). The grey shaded area is ruled out by the $B_s - \bar{B}_s$ mixing constraint. In the pink region, the required g_μ to fit the B anomalies is ruled out by neutrino trident production.

enhanced limits. Increasing $m_{Z'}$ improves on the relative reach of the inclusive dimuon search due to reducing SM background expectations. At $m_{Z'} = 1$ TeV, the current search limit does not rule out any parameter space although increasing integrated luminosities should facilitate large improvements. The projected inclusive dimuon resonance search will be able to probe some parameter space up to $m_{Z'} \sim 3$ TeV, where the cross section is too small even for 3000 fb^{-1}.

In summary, we pointed out that the fusion of b quarks from gluon splittings and sea-quark distributions at the LHC is vital for testing heavy Z' models where the Z' boson preferredly couples to quarks in the third generations. If such models are used to explain the B anomalies, we show that there is a lower limit on such production processes that arises from the flavor-violating bs coupling. Producing such a Z' in a final state is expected in association with one or two b jets. The presence of the resonance due to the BFF initiated processes allows us to probe such models in the inclusive searches. Furthermore, the presence of additional b jets along with kinematical requirements on them is found to be effective in reducing SM backgrounds in background-dominated search regions (e.g., ≤ 500 GeV for the 13 TeV LHC). The prospects for testing the entire parameter space of such models for some Z' masses appear to be complimentary in the existing and upcoming LHC program.

ACKNOWLEDGMENTS

M. A., B. D., R. E., T. K., D. R. and P. H. are supported in part by the DOE Grant No. DE-SC0010813. M. D., P. H., and A. T. thank the Mitchell Institute for Fundamental Physics and Astronomy for support. T. K. is also supported in part by Qatar National Research Fund under Project No. NPRP 9-328-1-066. We would like to thank A. Datta, T. Ghosh, Xiao-Gang He, M. L. Mangano, J. Ruderman and J. Walker for useful discussions and comments.

[1] S. Chatrchyan *et al.* (CMS Collaboration), Observation of a new boson at a mass of 125 GeV with the CMS experiment at the LHC, Phys. Lett. B **716**, 30 (2012).

[2] G. Aad *et al.* (ATLAS Collaboration), Observation of a new particle in the search for the Standard Model Higgs boson with the ATLAS detector at the LHC, Phys. Lett. B **716**, 1 (2012).

[3] R. Aaij *et al.* (LHCb Collaboration), Measurement of Form-Factor-Independent Observables in the Decay $B^0 \to K^{*0}\mu^+\mu^-$, Phys. Rev. Lett. **111**, 191801 (2013).

[4] R. Aaij *et al.* (LHCb Collaboration), Angular analysis of the $B^0 \to K^{*0}\mu^+\mu^-$ decay using 3 fb^{-1} of integrated luminosity, J. High Energy Phys. 02 (2016) 104.

[5] A. Abdesselam *et al.* (Belle Collaboration), in Proceedings, LHCSki 2016—A First Discussion of 13 TeV Results: Obergurgl, Austria, April 10-15, 2016. (2016) http://inspirehep.net/record/1446979/files/arXiv:1604.04042.pdf.

[6] M. Ciuchini, M. Fedele, E. Franco, S. Mishima, A. Paul, L. Silvestrini, and M. Valli, $B \to K^*\ell^+\ell^-$ decays at large recoil in the Standard Model: a theoretical reappraisal, J. High Energy Phys. 06 (2016) 116.

[7] R. Aaij *et al.* (LHCb Collaboration), Test of Lepton Universality Using $B^+ \to K^+\ell^+\ell^-$ Decays, Phys. Rev. Lett. **113**, 151601 (2014).

[8] R. Aaij *et al.* (LHCb Collaboration), Test of lepton universality with $B^0 \to K^{*0}\ell^+\ell^-$ decays, J. High Energy Phys. 08 (2017) 055.

[9] G. D'Amico, M. Nardecchia, P. Panci, F. Sannino, A. Strumia, R. Torre, and A. Urbano, Flavour anomalies after the R_{K^*} measurement, J. High Energy Phys. 09 (2017) 010.

[10] B. Capdevila, A. Crivellin, S. Descotes-Genon, J. Matias, and J. Virto, Patterns of new physics in $b \to s\ell^+\ell^-$ transitions in the light of recent data, J. High Energy Phys. 01 (2018) 093.

[11] R. Gauld, F. Goertz, and U. Haisch, An explicit Z'-boson explanation of the $B \to K^*\mu^+\mu^-$ anomaly, J. High Energy Phys. 01 (2014) 069.

[12] A. J. Buras and J. Girrbach, Left-handed Z' and Z FCNC quark couplings facing new $b \to s\mu^+\mu^-$ data, J. High Energy Phys. 12 (2013) 009.

[13] A. J. Buras, F. De Fazio, and J. Girrbach, 331 models facing new $b \to s\mu^+\mu^-$ data, J. High Energy Phys. 02 (2014) 112.

[14] A. Greljo, G. Isidori, and D. Marzocca, On the breaking of lepton flavor universality in B decays, J. High Energy Phys. 07 (2015) 142.

[15] W. Altmannshofer and I. Yavin, Predictions for lepton flavor universality violation in rare B decays in models with gauged $L_\mu - L_\tau$, Phys. Rev. D **92**, 075022 (2015).

[16] A. Crivellin, G. D'Ambrosio, and J. Heeck, Explaining $h \to \mu^\pm\tau^\mp$, $B \to K^*\mu^+\mu^-$ and $B \to K\mu^+\mu^-/B \to Ke^+e^-$ in a Two-Higgs-Doublet Model with Gauged $L_\mu - L_\tau$, Phys. Rev. Lett. **114**, 151801 (2015).

[17] A. Crivellin, G. D'Ambrosio, and J. Heeck, Addressing the LHC flavor anomalies with horizontal gauge symmetries, Phys. Rev. D **91**, 075006 (2015).

[18] C. Niehoff, P. Stangl, and D. M. Straub, Violation of lepton flavour universality in composite Higgs models, Phys. Lett. B **747**, 182 (2015).

[19] A. Falkowski, M. Nardecchia, and R. Ziegler, Lepton flavor non-universality in B-meson decays from a U(2) flavor model, J. High Energy Phys. 11 (2015) 173.

[20] B. Allanach, F. S. Queiroz, A. Strumia, and S. Sun, Z models for the LHCb and $g-2$ muon anomalies, Phys. Rev. D **93**, 055045 (2016); Erratum, Phys. Rev. D **95**, 119902(E) (2017).

[21] G. Blanger, C. Delaunay, and S. Westhoff, A dark matter relic from muon anomalies, Phys. Rev. D **92**, 055021 (2015).

[22] S. M. Boucenna, A. Celis, J. Fuentes-Martin, A. Vicente, and J. Virto, Phenomenology of an $SU(2) \times SU(2) \times U(1)$ model with lepton-flavour non-universality, J. High Energy Phys. 12 (2016) 059.

[23] C.-W. Chiang, X.-G. He, and G. Valencia, Z model for bs flavor anomalies, Phys. Rev. D **93**, 074003 (2016).

[24] B. Bhattacharya, A. Datta, J.-P. Guvin, D. London, and R. Watanabe, Simultaneous explanation of the R_K and $R_{D^{(*)}}$ puzzles: A model analysis, J. High Energy Phys. 01 (2017) 015.

[25] A. Crivellin, J. Fuentes-Martin, A. Greljo, and G. Isidori, Lepton flavor non-universality in B decays from dynamical Yukawas, Phys. Lett. B **766**, 77 (2017).

[26] A. K. Alok, B. Bhattacharya, A. Datta, D. Kumar, J. Kumar, and D. London, New physics in $b \to s\mu^+\mu^-$ after the measurement of R_{K^*}, Phys. Rev. D **96**, 095009 (2017).

[27] P. Ko, Y. Omura, Y. Shigekami, and C. Yu, The LHCb anomaly and B physics in flavored Z' models with flavored Higgs doublets, Phys. Rev. D **95**, 115040 (2017).

[28] C.-W. Chiang, X.-G. He, J. Tandean, and X.-B. Yuan, $R_{K^{(*)}}$ and related $b \to s\ell\bar{\ell}$ anomalies in minimal flavor violation framework with Z' boson, Phys. Rev. D **96**, 115022 (2017).

[29] J. Ellis, M. Fairbairn, and P. Tunney, Anomaly-free models for flavour anomalies, arXiv:1705.03447.

[30] Y. Tang and Y.-L. Wu, Flavor non-universality gauge interactions and anomalies in B-meson decays, Chin. Phys. C **42**, 033104 (2018).

[31] J. F. Kamenik, Y. Soreq, and J. Zupan, Lepton flavor universality violation without new sources of quark flavor violation, Phys. Rev. D **97**, 035002 (2018).

[32] F. Sala and D. M. Straub, A new light particle in B decays?, Phys. Lett. B **774**, 205 (2017).

[33] S. Di Chiara, A. Fowlie, S. Fraser, C. Marzo, L. Marzola, M. Raidal, and C. Spethmann, Minimal flavor-changing Z' models and muon $g-2$ after the R_{K^*} measurement, Nucl. Phys. **B923**, 245 (2017).

[34] R. Alonso, P. Cox, C. Han, and T. T. Yanagida, Anomaly-free local horizontal symmetry and anomaly-full rare B-decays, Phys. Rev. D **96**, 071701 (2017).

[35] C. Bonilla, T. Modak, R. Srivastava, and J. W. F. Valle, $U(1)_{B_3-3L_\mu}$ gauge symmetry as the simplest description of $b \to s$ anomalies, arXiv:1705.00915.

[36] S. Baek, Dark matter contribution to $b \to s\mu^+\mu^-$ anomaly in local $U(1)_{L_\mu - L_\tau}$ model, arXiv:1707.04573.

[37] R. Alonso, P. Cox, C. Han, and T. T. Yanagida, Flavoured *B-L* local symmetry and anomalous rare B decays, Phys. Lett. B **774**, 643 (2017).

[38] L. Bian, S.-M. Choi, Y.-J. Kang, and H. M. Lee, A minimal flavored $U(1)'$ for B-meson anomalies, Phys. Rev. D **96**, 075038 (2017).

[39] D. London and J. L. Rosner, Extra gauge bosons in E(6), Phys. Rev. D **34**, 1530 (1986).

[40] M. Cvetic and P. Langacker, New gauge bosons from string models, Mod. Phys. Lett. A **11**, 1247 (1996).

[41] M. Cvetic, D. A. Demir, J. R. Espinosa, L. L. Everett, and P. Langacker, Electroweak breaking and the mu problem in supergravity models with an additional U(1), Phys. Rev. D **56**, 2861 (1997); Erratum, Phys. Rev. D **58**, 119905(E) (1998).

[42] N. Arkani-Hamed, A. G. Cohen, and H. Georgi, Electroweak symmetry breaking from dimensional deconstruction, Phys. Lett. B **513**, 232 (2001).

[43] C. T. Hill and E. H. Simmons, Strong dynamics and electroweak symmetry breaking, Phys. Rep. **381**, 235 (2003); Erratum, Phys. Rep. **390**, 553(E) (2004).

[44] V. Khachatryan *et al.* (CMS Collaboration), Search for narrow resonances in dilepton mass spectra in proton-proton collisions at $\sqrt{s} = 13$ TeV and combination with 8 TeV data, Phys. Lett. B **768**, 57 (2017).

[45] ATLAS Collaboration CERN Technical Report No. ATLAS-CONF-2016-045, 2016; http://cds.cern.ch/record/2206127.

[46] A. M. Sirunyan (CMS Collaboration), Search for high-mass resonances in dilepton final states in proton-proton collisions at $\sqrt{s} = 13$ TeV, arXiv:1803.06292.

[47] W. Altmannshofer, P. Stangl, and D. M. Straub, Interpreting hints for lepton flavor universality violation, Phys. Rev. D **96**, 055008 (2017).

[48] D. Aristizabal Sierra, F. Staub, and A. Vicente, Shedding light on the $b \to s$ anomalies with a dark sector, Phys. Rev. D **92**, 015001 (2015).

[49] W. Altmannshofer, S. Gori, M. Pospelov, and I. Yavin, Quark flavor transitions in $L_\mu - L_\tau$ models, Phys. Rev. D **89**, 095033 (2014).

[50] ATLAS Collaboration, CERN Technical Report No. ATLAS-CONF-2016-030, 2016; http://cds.cern.ch/record/2161135.

[51] M. Aaboud *et al.* (ATLAS Collaboration), Search for resonances in the mass distribution of jet pairs with one or two jets identified as b-jets in proton–proton collisions at $\sqrt{s} = 13$ TeV with the ATLAS detector, Phys. Lett. B **759**, 229 (2016).

[52] A. M. Sirunyan *et al.* (CMS Collaboration), Search for dijet resonances in proton-proton collisions at $\sqrt{s} = 13$ TeV and constraints on dark matter and other models, Phys. Lett. B **769**, 520 (2017).

[53] V. Sanchez Martinez (ATLAS Collaboration), ATLAS $t\bar{t}$ resonance searches, Nucl. Part. Phys. Proc. **273–275**, 2814 (2016).

[54] V. Khachatryan *et al.* (CMS Collaboration), Search for resonant $t\bar{t}$ production in proton-proton collisions at $\sqrt{s} = 8$ TeV, Phys. Rev. D **93**, 012001 (2016).

[55] M. Bona (UTfit Collaboration), Unitarity triangle analysis beyond the standard model from UTfit, *Proc. Sci.*, ICHEP2016 (2016) 149.

[56] G. W. Bennett *et al.* (Muon g-2 Collaboration), Measurement of the Negative Muon Anomalous Magnetic Moment to 0.7 ppm, Phys. Rev. Lett. **92**, 161802 (2004).

[57] J. P. Lees *et al.* (*BABAR* Collaboration), Search for $B \to K^{(*)}\nu\bar{\nu}$ and invisible quarkonium decays, Phys. Rev. D **87**, 112005 (2013).

[58] O. Lutz *et al.* (Belle Collaboration), Search for $B \to h^{(*)}\nu\bar{\nu}$ with the full Belle $\Upsilon(4S)$ data sample, Phys. Rev. D **87**, 111103 (2013).

[59] W. Altmannshofer, S. Gori, M. Pospelov, and I. Yavin, Neutrino Trident Production: A Powerful Probe of New Physics with Neutrino Beams, Phys. Rev. Lett. **113**, 091801 (2014).

[60] J. Alwall, R. Frederix, S. Frixione, V. Hirschi, F. Maltoni, O. Mattelaer, H. S. Shao, T. Stelzer, P. Torrielli, and M. Zaro, The automated computation of tree-level and next-to-leading order differential cross sections, and their matching to parton shower simulations, J. High Energy Phys. 07 (2014) 079.

[61] C. Duhr, Hidden Abelian Higgs model., http://feynrules.irmp.ucl.ac.be/wiki/HiddenAbelianHiggsModel#no1.

[62] N. D. Christensen and C. Duhr, FeynRules—Feynman rules made easy, Comput. Phys. Commun. **180**, 1614 (2009).

[63] A. Alloul, N. D. Christensen, C. Degrande, C. Duhr, and B. Fuks, FeynRules 2.0—A complete toolbox for tree-level phenomenology, Comput. Phys. Commun. **185**, 2250 (2014).

[64] T. Sjstrand, S. Ask, J. R. Christiansen, R. Corke, N. Desai, P. Ilten, S. Mrenna, S. Prestel, C. O. Rasmussen, and P. Z. Skands, An introduction to PYTHIA 8.2, Comput. Phys. Commun. **191**, 159 (2015).

[65] J. de Favereau, C. Delaere, P. Demin, A. Giammanco, V. Lematre, A. Mertens, and M. Selvaggi (DELPHES 3 Collaboration), DELPHES 3, A modular framework for fast simulation of a generic collider experiment, J. High Energy Phys. 02 (2014) 057.

[66] C. G. Lester and D. J. Summers, Measuring masses of semiinvisibly decaying particles pair produced at hadron colliders, Phys. Lett. B **463**, 99 (1999).